



High sensitivity long pulse envelope detector assisted by microwave photonics

Detector de envoltória de pulso longo de alta sensibilidade assistido por micro-ondas em fotônica

André Paim Gonçalves^{1,*} , Felipe Streitenberger Ivo¹ , Olympio Lucchini Coutinho¹

1. Departamento de Ciência e Tecnologia Aeroespacial – Instituto Tecnológico de Aeronáutica – Divisão de Eletrônica – São José dos Campos (SP), Brazil.

Correspondence author: andreg43@yahoo.com.br

Section Editor: Álvaro Damião

Received: May 30, 2022 **Approved:** Sept. 21, 2022

ABSTRACT

This article presents a concept of a long pulse envelope detector with a high sensitivity value based on microwave photonics (MWP). The process of envelope detecting of radio frequency (RF) signals is achieved by the translation of the RF spectrum to the optical spectrum range followed by optical filtering to cut the lower sideband and the carrier, finally beating the remaining upper sideband into a low-speed photodetector (LSPD). The LSPD output signal is amplified by transimpedance gain. This approach depends only on the RF passing band of the phase modulator and the optical filter transfer function. This concept is experimentally demonstrated by reaching envelope detector tangential signal sensitivity (TSS) values around -40 dBm for RF input frequency range from 10 to 20 GHz. The proposed architecture does not use any optical or video signal amplifier. The implementation of this approach is simple, employs few components, and is commercial off-the-shelf.

KEYWORDS: RF power sensing, Self-homodyne detection, Electronic warfare.

RESUMO

Este artigo apresenta um conceito de detector de envelope de pulso longo com um alto valor de sensibilidade baseado em micro-ondas em fotônica (MWP). O processo de detecção de envelopes de sinais de radiofrequência (RF) é conseguido através da conversão do sinal de RF para a faixa do espectro óptico, seguido de filtragem óptica para eliminar a banda lateral inferior e a portadora, realizando o batimento das componentes espectrais da banda lateral superior num fotodetector de baixa velocidade (LSPD). O sinal de saída do LSPD é amplificado pelo ganho de transimpedância. Esta abordagem depende apenas da banda de passagem RF do modulador de fase e da função de transferência do filtro óptico. Este conceito é demonstrado experimentalmente ao atingir valores de sensibilidade do sinal tangencial (TSS) do detector de envelope em torno de -40 dBm para a faixa de frequências de entrada de RF de 10 a 20 GHz. A arquitetura proposta não utiliza qualquer amplificador de sinal óptico ou de vídeo. A implementação desta abordagem é simples, emprega poucos componentes e encontrados no comércio.

PALAVRAS-CHAVE: Detector de potência de RF, Detecção auto-homódina, Guerra eletrônica.

INTRODUCTION

With the advent of the great development of satellite link communications and cellular telephony, the electromagnetic environment has become very dense near large urban centers. Such a fact brings a huge difficulty for electronic warfare sensors employed near urban centers. With the dense electromagnetic environment, the receivers have a lot of problems separating the signals of interest from the others. When the signals of interest

become those from radars with a low probability of interception (LPI) this difficulty is aggravated thanks to their low signal-to-noise ratio (SNR) in the electronic warfare receiver and their large pulse width^{1,2}. When the large SNR signals with smaller pulse lengths arrive at the same time as signals from radars with LPI characteristics, electronic warfare receivers have big difficulty detecting and separating these two types of signals. Electronic warfare system designers have been seeking to solve the problem of detecting radar signals with LPI characteristics by increasing the sensitivity of receivers and employing fast devices to be able to differentiate between signals incident at the same time on electronic warfare receivers, especially those of long duration^{1,2}.

Techniques employed to solve the problem of overlapping long-duration and low SNR signals have been based on digital signal processing of microwave signals, but performance is still limited due to the low sampling speed relative to the frequency bands required in modern radars³.

An alternative approach to the problem is MWP. This is an area of human knowledge that emerged in the 1970s and employs optical energy to generate, transmit, and process RF signals. The MWP aims to overcome some limitations suffered by electronics in terms of RF bandwidth, larger RF carriers, volume, weight, power consumption, and response speed⁴.

The purpose of this paper is to point out the possibilities and limitations of using MWP to solve the problem of detecting signals with low SNR and overlapping long signals with short signals in duration.

METHODS

System configuration and principle

The principle of operating the fully photonic envelope detector is shown in Fig. 1. The laser light wave is coupled to the phase modulator and undergoes optical phase modulation by the RF signal. The modulated optical signal passes through an optical filter. The theoretical carrier and the lower sideband of the modulated signal are rejected. The upper sideband portion of the modulated optic signal is transmitted through the filter to the photodetector, to be converted into a baseband electrical signal by direct detection. This process is similar to the one used by Hossein-Zadeh and Levi⁵, where the authors presented this structure as a down converter for an ultra-wideband (UWB) receiver.

There are two important processes to consider in the proper operation of this system. The first is the conversion of the phase to intensity optic modulation. The optical phase-modulated has an optical carrier and lower sideband filtered, only the upper sideband coupled to the photodetector. Figure 2 illustrates how this filtering is done. The most common process is the use of an optical filter to eliminate one of the lateral sidebands of the modulated signal and inject the optical carrier and the remaining sideband into the photodetector⁶. The second process is self-homodyne detection. The upper sideband frequency components beat themselves. If a low-speed photodetector (LSPD) is chosen, it works like a low pass filter, because the RF output response is low frequency and its equivalent circuit is a current source with load in parallel junction capacitance, like in Fig. 1. The result of this process is the detection of the RF pulse envelope. The LSPD equivalent circuit behavior allows transimpedance gain in the output signal.

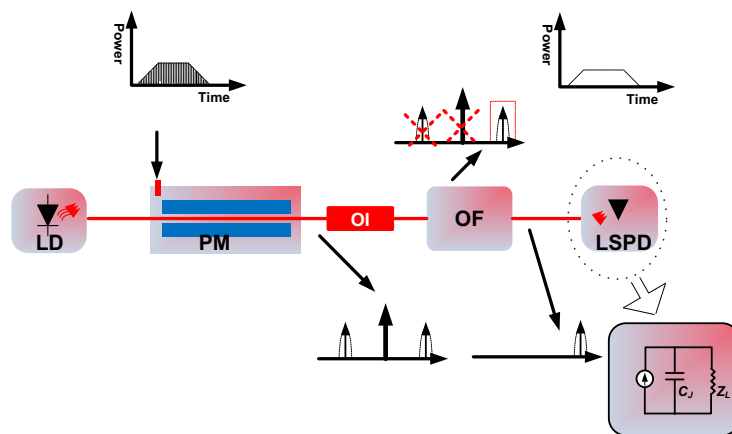


Figure 1: Schematic diagram of the photonic envelope detector.

LD: laser diode; PM: phase modulator; OI: optical isolator; OF: optical filter; LSPD: low-speed photodetector; C_j : junction capacitance; Z_L : output load.

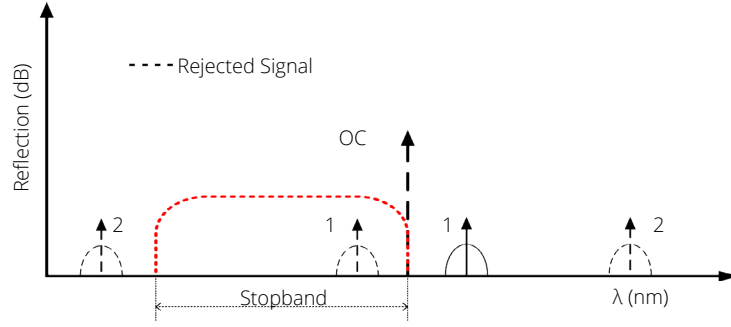


Figure 2: Schematic diagram of the behavior of the optical filter and the optical carrier tuning.
OC: optical carrier; 1 and 2 mean the sidebands of the optical signal modulated at the optical filter.

RESULTS AND DISCUSSION

Mathematical modeling of the photonic envelope detector

An optical electric field of laser carrier can be expressed by Eq. 1:

$$E(t)_o = E_o \exp[j(\omega_o t + \varphi_i)] \quad (1)$$

where E_o is the electric field amplitude of the signal coming from the laser diode.

Let us consider an electrical RF signal feeding the RF input of a phase modulator defined as Eq. 2:

$$V(t)_{RF} = V[\cos[(\omega_{RF} + \Delta\omega_{RF})t + \varphi_{RF}] + \cos[(\omega_{RF} - \Delta\omega_{RF})t + \varphi_{RF}]] \quad (2)$$

where V is the amplitude of the incident RF voltage, ω_{RF} is the angular frequency, and φ_{RF} is the RF phase. The $\Delta\omega_{RF}$ is the instantaneous RF pulse bandwidth divided by two.

In the phase modulator, the optical carrier undergoes a phase change expressed by Urick et al.⁶ (Eq. 3):

$$E(t)_o = \{E_o \exp[j\omega_o t] \times \exp[jm \cos[(\omega_{RF} + \Delta\omega_{RF})t + \varphi_{RF}]] \times \exp[jm \cos[(\omega_{RF} - \Delta\omega_{RF})t + \varphi_{RF}]]\} \quad (3)$$

The modulation index m is defined in Eq. 4⁶:

$$m = \frac{V}{V_\pi} \pi \quad (4)$$

where the V_π is the half-wave voltage of the phase modulator.

The phase modulator output is described by Eq. 3 and becomes Eq. 5 when the Jacobi-Anger is applied, considering a small RF signal operating regime, where $m \ll 1$, and the filter transmission frequency response is described by transmission coefficient $T(\omega)$ and phase $\varphi(\omega)$. The RF filter tuning caused the optic carrier and its lower sideband elimination ($T(\omega) = 0$) as shown in Fig. 2.

$$E(t)_i \approx T(\omega) E_i J_1(m) \times \{ \exp[j[(\omega_o + \omega_{RF} + \Delta\omega_{RF})t + \varphi_{RF} + \pi/2 + \varphi(\omega)]] + \exp[j[(\omega_o + \omega_{RF} - \Delta\omega_{RF})t + \varphi_{RF} + \pi/2 + \varphi(\omega)]] \} \quad (5)$$

The $J_1(m)$ is Bessel function of the first kind of order 1. The $T(\omega)$ and $\varphi(\omega)$ parameters were considered as and at the out of the stopband region. The optic signal described by Eq. 5 becomes Eq. 6 due to the frequency component beating at PD. The current value at PD output described by Eq. 6 is found by calculating the value of the Poynting vector module and applying some algebraic processes. The alternated current value is estimated by Eq. 6:

$$i(t) = 2\Re(TP_o J_1(m))^2 \cos(2\Delta\omega_{RF} t) \quad (6)$$

where \mathfrak{R} is the PD responsivity, and P_o is the optic power at input system, where is $P_o \sim E_o^2$.

Observing Eq. 6, it is possible to realize that the electric signal at the photodetector output is the baseband signal of the RF phase modulator input. The result is the envelope of the input signal converted to current at the photodetector output. Faced with this fact, this architecture can explore LSPD, that is, photodetector with output band in the baseband, a few kHz. With the signal band in the order of kHz, it becomes possible to implement transimpedance gain with the increase of the load on the device output. The PD output voltage value (V_{out}) was estimated according to Eq. 6 and Table 1. The carrier frequency considered was 17 GHz and the losses values were 8.9 dB.

Table 1: The theoretical PRF values.

P_{RF} (mW)	P_o (mW)	\mathfrak{R} (W/A)	V_π (V)	Z_L (M Ω)	i (μ A)	V_{out} (V)
0.59	100	1	10.5	1	22.9	22.9
0.01	100	1	3.5	1	35.0	35.0
0.001	100	1	0.35	1	35.0	35.0

The performance of the envelope detector can be improved by reducing the value of V_π according to Eq. 6, and increasing the load impedance^{5,7,8}. The value of V_π can reach 0.3 V_π when an electro-optical polymer modulator was used⁹.

Experimental demonstration of the photonic envelope detector tangential signal sensitivity (TSS)

To demonstrate and measure the TSS of the photonic envelope detector, an experiment was carried out. The schematic diagram is shown in Fig. 3. A distributed feedback laser (DFB) laser is used as an optical source. The phase modulator operates at frequencies up to 20 GHz. A uniform fiber Bragg grating (FBG) was used as an optical filter followed by a 1.5 GHz LSPD. The RF signal generator is used to perform the pulse radar signal and a high-speed digital sampling oscilloscope is used to measure the input RF modulated signal and the output video signal, that is, the envelope of the input signal.

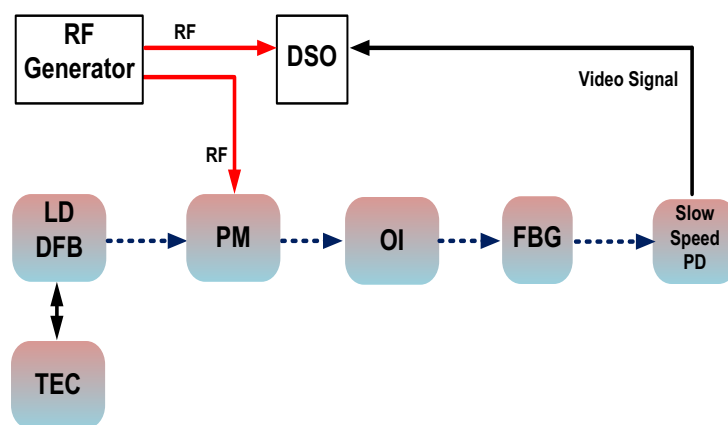


Figure 3: Schematic diagram setup of the receiver.

DFB: distributed feedback laser; TEC: thermal electronic cooler; PM: phase modulator; OI: optical isolator; RF: radio frequency; PD: photodetector; FBG: fiber Bragg grating.

The uniform optical FBG was chosen as an optic filter. For the sake of simplicity, Fig. 4 shows only the right side of the rejection passband optical filter, cut right on the center frequency. The right edge has a roll-off starting from the total transmission and ending at the beginning of the region's maximum optical signal reflection.

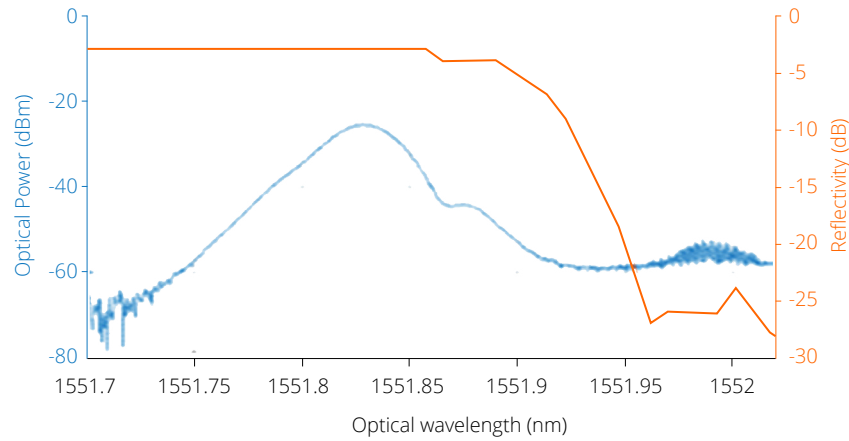


Figure 4: The right side of the rejection passband optical filter is shown. The cut right on the center frequency is represented by an orange line. This center is around 1551.71 nm. The blue dotted line represents an optical signal modulated by an RF pulsed signal with power equal to -40 dBm.

The optical carrier and lower sideband were reduced drastically according to Fig.4. The transition region between the stopband and transmission band has a roll-off of around $2.86 \text{ dB}\cdot\text{GHz}^{-1}$ according to Fig. 4. This imposes a limitation on the flatness of RF response operation band, starting at 10 GHz, considering the laser carrier tuned at frequency right on the edge of the optic stopband.

The envelope detector tuning occurs as explained previously. The TSS measuring was performed with laser tuning according presented in Fig. 4, and then applying a pulsed RF signal at the phase modulator input and varying its frequency from 0 to 20 GHz. Laser power was 100 mW and the system had 8.9 dB as optical losses. The photodetector load impedance is 1000 k Ω . The minimum pulse width was 4 ms and the pulse repetition interval chosen was equal to 10 ms. When the LSPD load is changed to 27 k Ω , the minimum pulse width was 25 μs and the pulse repetition interval chosen was equal to 100 μs . The RF pulses input are shown in the upper part of the figure and the baseband pulses are observed in the lower part in Fig. 5. The TSS measuring was performed by RF power variation at phase modulator input. The RF power was decreased until the output video power signal is 8 dB above the noise level¹⁰.

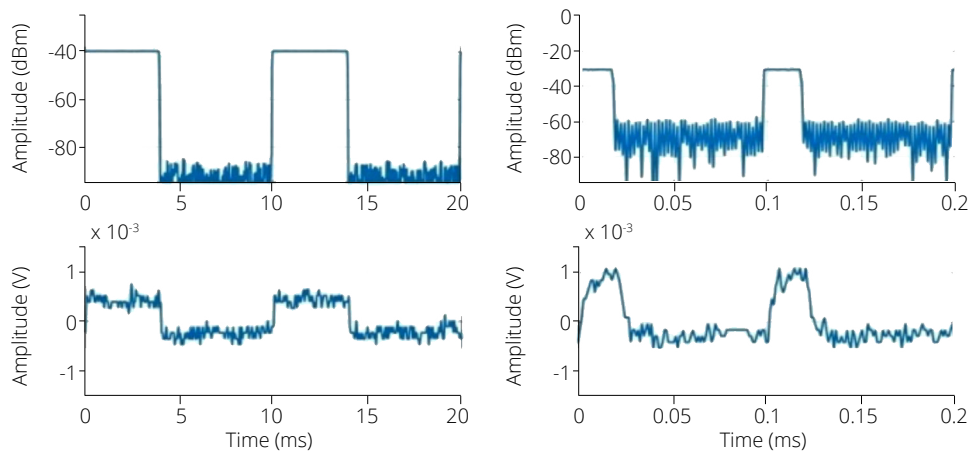


Figure 5: The RF input signals power at 17 GHz are shown in the superior part of the figure. The pulse widths of the RF signals are 4 ms and 25 μs from the left side respectively. The lower part of the figure show video signals voltage at 8 dB condition for TSS measuring.

The RF minimum input power was -40 dBm when the LSPD load was 1,000 k Ω and -30 dBm when the LSPD load was 27 k Ω . When the RF signal power is set at -40 dBm, it produces a modulation index equal to 9.46×10^{-4} . The TSS decreased because the transimpedance decreased. The flatness test was performed with an LSPD load equal to 1,000 k Ω and the RF power at phase modulator input is equal to -40 dBm, the RF frequency value varied from 1 to

20 GHz. We perceived that the TSS decreases when the pulsed signal RF frequency carrier varies from 1 to 10 GHz. This fact occurs due to there is a roll-off of the Bragg grating response. If the V_{π} value is 0.35 V and the modulated index is 9.46×10^{-4} (the same value achieved at TSS equal to -40 dBm for V_{π} equal to 10.5 V for frequency of 17 GHz), the TSS value will be around -69 dBm.

The video signal cut frequency depends on the load at LSPD output and the junction capacitance. When the load value is equal to 1,000 k Ω , the cut frequency is around 250 Hz and allows a pulse width of around 4 ms. The cut frequency value is around 40 kHz and the pulse width is around 25 μ s for a load value equal to 27 k Ω . The junction capacitance value is equal for both cases.

CONCLUSION

This article presented a microwave photonic approach to RF envelope detection for long pulses. As this system uses an optic phase modulator, it does not need to use a bias voltage controller circuit compared with the others those use intensity modulators.

The approach presented in this work is implemented with a few simple components, these characteristics can improve the reliability of the system, as well as reduce weight, power consumption, and size. It has the possibility of miniaturization of the optical circuit, which would facilitate its use in aerospace applications. The photonic envelope detector TSS reaches -40 dBm and can be around -70 dBm for a V_{π} value equal to 0.35 V. The photonic envelope detector can be more sensitive than a conventional one. However, the output voltage of the photonic envelope detector has decreasing values from 1 to 10 GHz and flat response from 10 to 20 GHz due to FBG roll-off. If the FBG has a roll-off better than 2.86 dB·GHz⁻¹ the response to be flatter. The LSPD has an equivalent circuit composed of a current source parallel to load and junction capacitance. This circuit behaves like a low passband filter. The system can be more sensitive to long-duration pulsed signals. In a dense electromagnetic environment, it can be an advantage. This fact occurs on account of the transimpedance gain; it limits the cut frequency at LSPD output. The transimpedance gain can be improved by using LSPD with junction capacitance lower than used at this approach and load increasing for the same cut frequency.

This system can detect LPI signals if improved because it can present a TSS value of around -70 dBm for long-duration pulses and it has short pulse filtering. The sensibility can be improved by RF preamplification at phase modulator input.

AUTHORS' CONTRIBUTIONS

Conceptualization: Gonçalves AP; **Methodology:** Gonçalves AP, Ivo FS and Coutinho OL; **Validation:** Gonçalves AP and Coutinho OL; **Formal analysis:** Gonçalves AP and Coutinho OL; **Investigation:** Gonçalves AP and Coutinho OL; **Resources:** Coutinho OL; **Data Curation:** Gonçalves AP and Ivo FS; **Writing - Original Draft:** Gonçalves AP; **Writing - Review & Editing:** Coutinho OL; **Visualization:** Gonçalves AP; **Supervision:** Coutinho OL; **Project administration:** Coutinho OL.

DATA AVAILABILITY STATEMENT

Data sharing is not applicable.

FUNDING

Coordenação de Aperfeiçoamento de Pessoal de Nível Superior
<https://doi.org/10.13039/501100002322>
Finance Code 001

ACKNOWLEDGEMENTS

Not applicable.

REFERENCES

1. Ruffe LI, Stott GF. LPI considerations for surveillance radars. 92 International Conference on Radar, 1992 Oct 12-13; Brighton, UK. p. 200-2.
2. De Martino A. Introduction to modern EW systems. 2nd ed. Artech House; 2018.
3. Pace PE. Detecting and classifying low probability of intercept radar. Artech House; 2009.
4. Capmany J, Novak D. Microwave photonics combines two worlds. *Nature Photon.* 2007;1:319-30. <https://doi.org/10.1038/nphoton.2007.89>
5. Hossein-Zadeh M, Levi AFJ. Selfhomodyne photonic microwave receiver architecture based on linear optical modulation and filtering. *Microw Opt Technol Lett.* 2008;50(2):345-50. <https://doi.org/10.1002/mop.23065>
6. Urick VJ, McKinney JD, Williams KJ. Fundamentals of microwave photonics. (Wiley Series in Microwave and Optical Engineering). Wiley; 2015.
7. Ziemer RE, Tranter WH. Principles of communications: Systems, modulation, and noise. 7th ed. John Wiley & Sons; 2015.
8. Lipsky SE. Microwave passive direction finding. SciTech; 2004.
9. Liu J, Xu G, Liu F, Kityk I, Liu X, Zhen Z. Recent advances in polymer electro-optic modulators. *RSC Advances.* 2015. <https://doi.org/10.1039/c4ra13250e>
10. Zahid M, Hussain I, Iqbal MF. Realistic estimation of signal-to-noise ratio in microwave receivers. 2019 16th International Bhurban Conference on Applied Sciences and Technology (IBCAST), 2019 Jan 08-12. Islamabad, Pakistan. p. 952-5. <https://doi.org/10.1109/IBCAST.2019.8667117>